J. of Cardiovasc. Trans. Res.
DOI 10.1007/s12265-015-9638-0

Variability of Mouse Left Ventricular Function Assessment by 11.7 Tesla MRI

Laetitia Vanhoutte[1,2,3] · Bernard Gallez[2] · Olivier Feron[3] · Jean-Luc Balligand[3] · Hrag Esfahani[3] · William d'Hoore[4] · Stéphane Moniotte[1]

Received: 9 April 2015 / Accepted: 2 June 2015

Abstract We studied intraobserver (n=24), interobserver (n=24) and interexperiment (n=12) reproducibility of left ventricular (LV) mass and volume measurements in mice using an 11.7 T MRI system. The LV systolic function was assessed with a short-axis FLASH-cine sequence in 29 mice, including animals having undergone transverse aortic constriction. Bland-Altman and regression analysis were used to compare the different data sets. Reproducibility was excellent for the LV mass and end-diastolic volume (coefficient of variability (CoV) between 5.4 and 11.8 %), good for end-systolic volume (CoV 15.2–19.4 %) and moderate for stroke volume and ejection fraction (CoV 14.7–20.9 %). We found an excellent correlation between LV mass determined by MRI and ex vivo morphometric data (r=0.92). In conclusion, LV systolic function can be assessed on an 11.7 T MRI scanner with high reproducibility for most parameters, as needed in longitudinal studies. However, data should be interpreted taking into account the moderate reproducibility of small volumes.

Keywords Mice · Ultra-high-field MRI · Systolic function · Reproducibility · Cardiac hypertrophy

Editor-in-Chief Jennifer L. Hall oversaw the review of this article

✉ Laetitia Vanhoutte
laetitia.vanhoutte@uclouvain.be

Bernard Gallez
bernard.gallez@uclouvain.be

Olivier Feron
olivier.feron@uclouvain.be

Jean-Luc Balligand
jl.balligand@uclouvain.be

Hrag Esfahani
hrag.esfahani@uclouvain.be

William d'Hoore
william.dhoore@uclouvain.be

Stéphane Moniotte
stephane.moniotte@uclouvain.be

[1] Division of Paediatric Cardiology, Department of Paediatrics, Cliniques Universitaires St. Luc, Université Catholique de Louvain (UCL), Avenue Hippocrate 10/1380, B-1200 Brussels, Belgium

[2] Biomedical Magnetic Resonance Unit (REMA), Louvain Drug Research Institute (LDRI), UCL, Brussels, Belgium

[3] Pole of Pharmacology and Therapeutics (FATH), Institute of Experimental and Clinical Research (IREC), UCL, Brussels, Belgium

[4] Institute for Health and Society (IRSS), UCL, Brussels, Belgium

Abbreviations

CMR	Cardiovascular magnetic resonance
CoV	Coefficient of variability
EDV	End-diastolic volume
EF	Ejection fraction
ESV	End-systolic volume
FLASH	Fast low angle shot
LV	Left ventricle
SV	Stroke volume
TL	Tibial length

Introduction

With heart diseases as the leading cause of morbidity and mortality in Western countries, cardiovascular research remains the prime importance in the field of scientific research [1]. In this context, recent developments in genetic, surgical and pharmacological modalities have led to a wider selection of animal models, especially small rodents, allowing us to better understand the underlying mechanisms of

Published online: 13 June 2015

cardiovascular diseases and to study new therapeutic interventions. However, characterization of the mouse cardiac phenotype remains challenging because of a small heart size—myocardial mass is 2000-fold smaller than human [2]—and rapid heart rate (400–600 beats/min).

The development of high-field MRI offers a valuable alternative to high-frequency echocardiography because of its potential higher reproducibility, the numerous imaging sequences available allowing specific investigations (biventricular function, fibrosis and viability, wall motion abnormalities) as well as the relatively non-invasive aspect of the technique, making it ideal for longitudinal monitoring of small animals [2–8]. Over time, the progression of the magnetic field strength of MRI scanners, from 3 to 11.7 T, has led to a better signal-to-noise ratio and an improvement of the spatial and temporal resolution. There are currently more than 40 MR systems installed worldwide operating at 7 T or higher [9].

Even if regularly used to study experimental models of cardiovascular diseases, data related to the reproducibility of left ventricular systolic function assessment in mice with these high-field magnets are limited. To our best knowledge, studies existing either used very small groups of animals ($n<10$) [10–12], only rats [12, 13], field strength under 7 T [14] or vertical bores [11–13]. They further only focused on the intra- and interobserver reproducibility or compared segmentation techniques [14, 15]; only one study by Stuckey et al. reported interexperimental reproducibility data on a group of 12 rats [13].

Such data are crucial to establish whether this technique is routinely applicable to mouse models, especially in dynamic studies using repeated acquisitions [16], and to determine how it compares to high-frequency echocardiographic analysis. In this study, our goals were to evaluate the intraobserver, interobserver and interexperiment variability of left ventricular (LV) mass and volumes in mice with an 11.7 T horizontal bore MR system and to compare these MRI data with ex vivo morphometric measurements.

Methods

Animals

29 C57Bl/6J male mice (Janvier, Paris) aged 10–28 weeks were studied. Mice were housed under standard conditions with ad libitum access to water and chow.

Surgical Procedures

Eleven mice have undergone minimally invasive transverse aortic constriction (TAC) to produce various degrees of cardiac hypertrophy [17, 18] in order to study the experimental variability of the technique in a wider range of physiopathological conditions (namely, with a wider spectrum of LV hypertrophy).

Mice were anaesthetized with an intraperitoneal injection of a mixture of ketamine (150 mg/kg) and xylazine (10 mg/kg) and placed in supine position. Under a microscope, an incision was performed on the right side of the sternum in order to avoid injury to the mammary artery. The thymus was pushed aside, and a constrictive band was placed and tightened around the aorta and a 27-G blunted needle, which was then removed. The ligature was not tightened in sham-operated mice. Chest was closed with a polypropylene suture. Thirteen mice were used as sham animals, and another 5 were control mice, for a total of 29 animals studied.

CMR Image Acquisition

Experiments were performed on an 11.7 T MRI system dedicated to small animal applications (Biospec, Bruker, Ettlingen, Germany). A quadrature ^{1}H resonator was used for radiofrequency transmission (inner diameter=72 mm, length=6.6 cm) in conjunction with a surface receive-only coil array (length=10.7 cm). All animals underwent at least one MRI examination. In the previously operated mice, the imaging took place 8 weeks after the surgical procedure. In 12 animals, the procedure was repeated twice, with a maximum interval of 24 h.

The animals were anaesthetized in an induction chamber by exposure to isoflurane 3 %. The isoflurane was then maintained between 0.5 and 3 % during the entire procedure in order to get a steady cardiac frequency around 500 beats/min [19]. Mice were placed in prone position and monitored for electrocardiogram and respiration with neonatal electrodes wrapped around the paws and a specific pillow placed under the animal. Examinations were performed in a temperature-controlled setting, with a rectal probe and a dedicated heating blanket.

Cardiac scout images were obtained in the conventional planes with a tripilot sequence. An intragate 2D cine Fast Low Angle Shot (FLASH) sequence was applied to acquire a set of seven to eight 1-mm-thick contiguous short-axis images covering the entire ventricles, perpendicular to the LV long axis. The following parameters were set: repetition time, 5.83 ms; echo time, 1.45 ms; flip angle, 25°; field of view, 30.0×30.0 mm; and matrix size, 256×256, resulting in an in-plane resolution of 0.12×0.12 mm^2, with an acquisition time of approximately 9 min, and 10 frames per cardiac cycle.

CMR Image Analysis

The LV systolic function was assessed from the stack of short-axis images by tracing epicardial and endocardial borders, including papillary muscles, on the Segment software (Medviso®v1.8, Lund, Sweden) [20]. End-diastolic (EDV), end-systolic (ESV) and stroke volume (SV) were determined

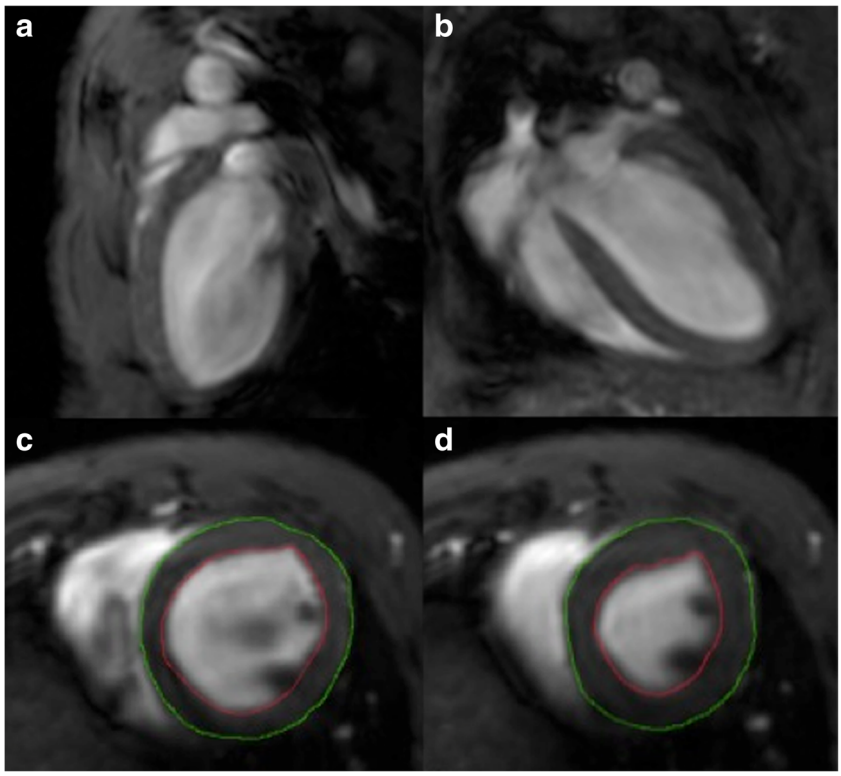

Fig. 1 Representative vertical long axis (**a**), horizontal long axis (**b**), and end-diastolic (**c**) and end-systolic (**d**) short-axis images in mice, with endocardial (*red*) and epicardial (*green*) outlines

(μl). LV ejection fraction (EF, in %) and LV mass (mg) were subsequently deduced. Twenty-four stacks of images were read twice by the same observer and once by an independent observer. The 24 series of images resulting from repeated acquisitions on the same animals were read by the first observer. The average time for image post-processing was about 15 min per animal. All analyses were performed on a blinded basis.

Morphometric Measurements

One week after the MRI procedure, mice were sacrificed. Their body weight, heart weight, left ventricular mass and tibial length (TL) were measured.

Statistical Analysis

Since most data were treated retrospectively, the 29 animals studied have not all been included in the various analysis groups. For intra- and interobserver variability, the same 24 mice were studied, including 13 sham and 11 TAC animals. For interexperiment variability, 12 animals were studied, including 3 sham, 4 TAC (also included in the intra- and interobserver analysis) and 5 control animals.

For intraobserver variability, the same stack of images was read twice by the same observer (data sets 1 and 1′). For interobserver variability, the same stack of images was read blindly by two independent observers (data sets 1 and 2). For interexperiment variability, two different stacks of images

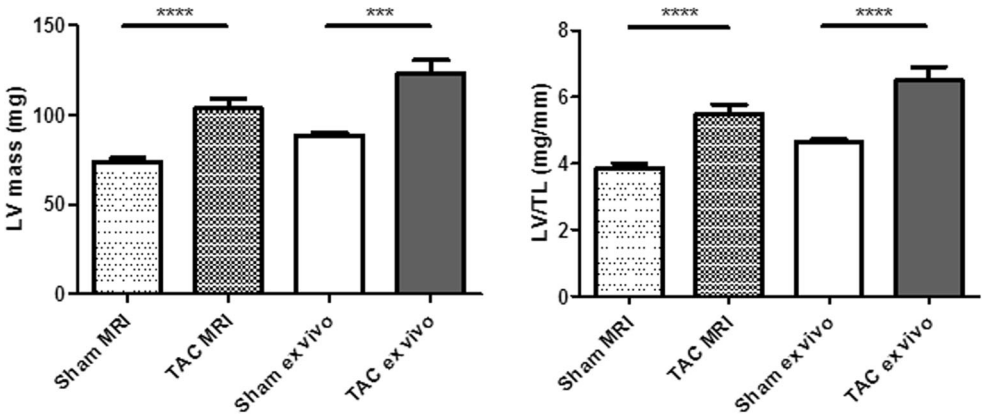

Fig. 2 Mass (mg) and LV/TL ratio (mg/mm) in sham and TAC mice assessed by MRI or ex vivo morphometric measurements. MRI data are issued from the first reading (data set 1). ***$P \leq 0.001$; ****$P \leq 0.0001$ vs sham

Table 1 Cardiac function and LV mass of sham and TAC mice. MRI data are issued from the first reading (data set 1)

	Sham	TAC
n	13	11
Body weight (g)	28.2±0.3	27.8±0.5
LV mass ex vivo (mg)	88.7±1.6	122.8±7.7***
LV/TL ex vivo (mg/mm)	4.7±0.1	6.5±0.4****
LV mass MRI (mg)	73.5±2.4	103.6±5.7****
LV/TL MRI (mg/mm)	3.9±0.1	5.5±0.3****
Heart rate (bpm)	496.6±11.1	509.5±11.3
EDV (μl)	60.1±2.4	76.1±5.4**
ESV (μl)	23.2±1.6	45.8±5.5***
SV (μl)	36.5±1.9	30.4±1.8*
EF (%)	61.2±2.0	41.6±3.7****
CO (ml/min)	18.1±0.9	15.4±0.8*

n represents the number of animals in each group. *EDV* end-diastolic volume, *ESV* end-systolic volume, *SV* stroke volume, *EF* ejection fraction, *CO* cardiac output

*$P \leq .0.05$; **$P \leq .0.01$; ***$P \leq .0.001$; ****$P \leq 0.0001$ vs sham

acquired in the same animal were read by the first observer (data sets 3 and 3′).

The mean and standard deviation of each parameter were computed in each group. Agreement between intraobserver, interobserver and interexperiment measurements was assessed by means of the Bland and Altman test [21] that plots the difference between the two measurements against the average of the two methods. The bias corresponds to the mean difference. The limits of agreement were estimated using the mean bias between the two readings plus or minus twice the standard deviation of the differences (SDD). The difference between the two measurements will be within these limits for 95 % of observations. The coefficient of variability (CoV) corresponds to the SDD divided by the mean of the measurements and multiplied by 100 %. It represents the percentage of dispersion of the measurements.

Unpaired Student's *t* test was used for intergroup comparison, including a comparative analysis of morphological and functional data (MRI data set 1) obtained for sham ($n=13$) and TAC mice ($n=11$). Paired *t* test was used to compare intraobserver, interobserver and interexperiment results for each parameter.

Table 2 Intraobserver, interexperiment and interobserver variability for LV mass (mg), LV/TL ratio (mg/mm), EDV (μl), ESV (μl), SV (μl) and EF (%). The table lists the mean±SD values and the Bland-Altman analysis results. Numbering of the data is organized as follows: 1 and 3 correspond to the first readings, 1′ is the reading of the same stack of images by the same observer (intraobserver), 2 is the reading of the same stack of images by an independent observer (interobserver) and 3′ corresponds to the reading of a second stack of images acquired on the same animal by the first observer (interexperiment)

Intraobserver variability ($n=24$)	LV mass	LV/TL	EDV	ESV	SV	EF
Mean±SD data #1	87.3±4.2	4.6±0.2	67.4±3.2	33.6±3.5	33.7±1.4	52.2±2.8
Mean±SD data #1	86.2±4.1	4.5±0.2	68.2±3.3	34.7±3.7	33.4±1.8	50.9±3.2
Bias	−1.1	−0.1	0.8	1.1	−0.3	−1.3
Limits of agreement	−10.4 to 8.1	−0.6 to 0.4	−6.4 to 7.9	−9.1 to 11.3	−10.4 to 9.7	−16.8 to 14.1
SDD	4.7	0.2	3.6	5.2	5.1	7.9
Coefficient of variability	5.4 %	5.4 %	5.4 %	15.2 %	15.3 %	15.3 %
Intraobserver variability ($n=24$)	LV mass	LV/TL	EDV	ESV	SV	EF
Mean±SD data #1	87.3±4.2	4.6±0.2	67.4±3.2	33.6±3.5	33.7±1.4	52.2±2.8
Mean±SD data #2	91.5±4.4	4.8±0.2	61.8±3.0	29.1±2.9	32.8±1.0	55.0±2.4
Bias	4.1	0.2	−5.6	−4.5	−0.9	2.8
Limits of agreement	−6.0 to 14.2	−0.3 to 0.8	−17.3 to 6.1	−16.4 to 7.4	−12.7 to 10.9	−12.7 to 18.3
SDD	5.1	0.3	6.0	6.1	6.0	7.9
Coefficient of variability	5.8 %	5.9 %	9.2 %	19.4 %	18.1 %	14.7 %
Interexperiment variability ($n=12$)	LV mass	LV/TL	EDV	ESV	SV	EF
Mean±SD data #3	83.5±5.8	4.3±0.4	72.6±4.2	35.4±5.5	37.1±2.3	53.4±4.5
Mean±SD data #3	87.3±5.7	4.5±0.4	70.2±4.6	34.2±6.0	35.8±2.7	53.9±5.0
Bias	3.8	0.2	−2.4	−1.3	−1.3	0.5
Limits of agreement	−9.3 to 16.8	−0.5 to 0.9	−18.9 to 14.1	−12.7 to 10.2	−16.2 to 13.7	−13.9 to 14.9
SDD	6.6	0.4	8.4	5.8	7.6	7.4
Coefficient of variability	7.8 %	8.3 %	11.8 %	16.8 %	20.9 %	15.5 %

n represents the number of animals studied

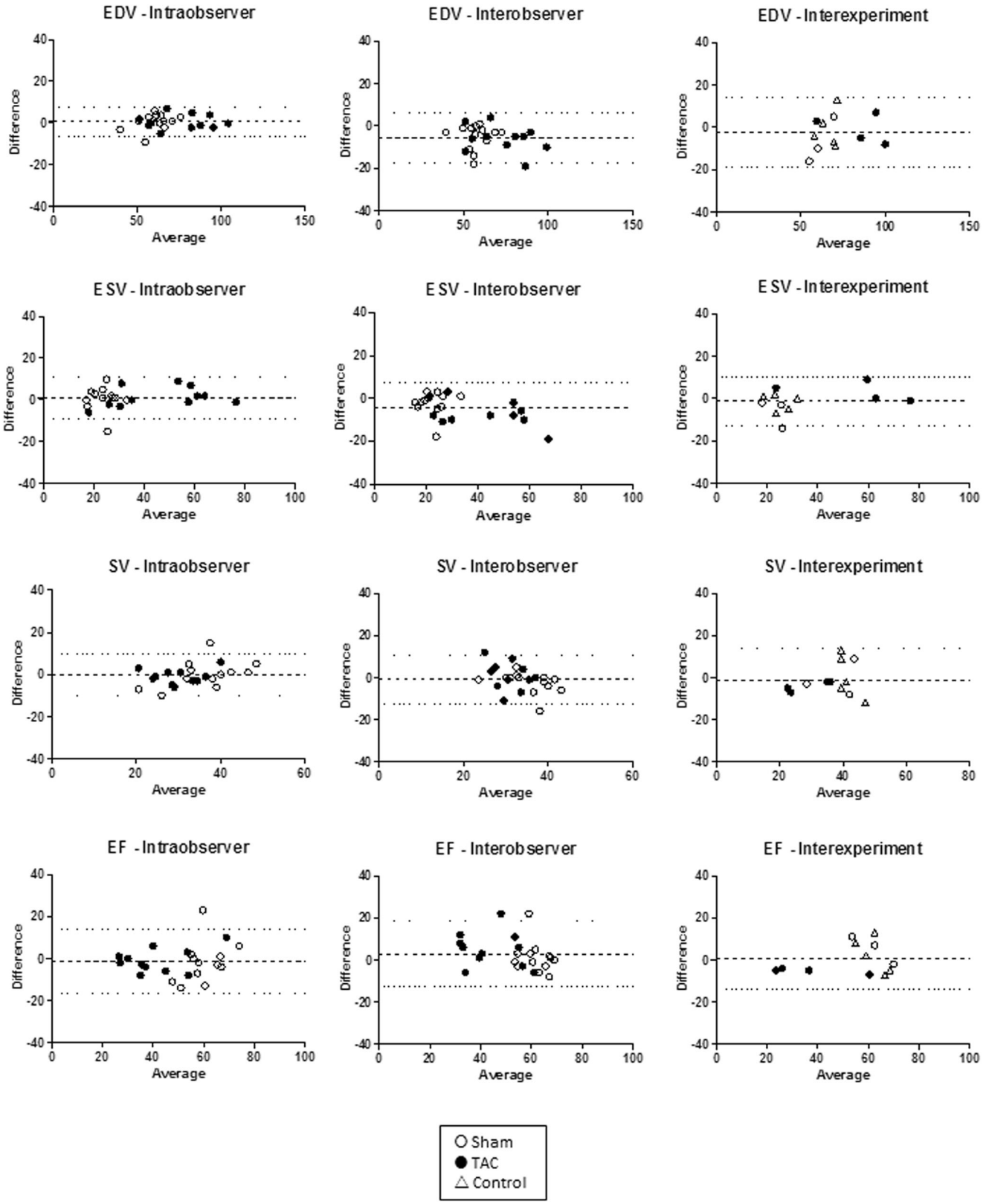

Fig. 3 Bland-Altman plots for EDV, ESV, SV and EF, assessing the agreement between the readings (interobserver, intraobserver and interexperiment). The relative variability is defined as the difference between observations divided by their mean. The *dashed lines* indicate the mean difference, while *dotted lines* indicate 95 % limits of agreement. All measurements showed a rather similar agreement of these main four parameters, not only in intra- or interobserver experiments (*left and central column*) but also in interexperiment analyses (*right column*)

A Pearson correlation was calculated in order to compare in vivo MRI data (data set 2) and ex vivo morphometric measurements of the LV mass and LV/TL ratio for the 13 sham and 11 TAC animals. A p value of <0.05 was considered statistically significant. Statistical analyses were performed with GraphPad Prism 5 (San Diego, USA).

Results

Using the CMR imaging protocol described above, high-grade quality images were obtained in all animals (Fig. 1).

Baseline Characteristics

Quantitative data were in line with previously published results [10, 11, 14–16, 19]. As expected, LV mass was significantly higher in the 11 animals with transverse aortic constriction and hypertrophic cardiomyopathy than in the 13 sham animals. When using the LV mass/tibial length ratio (LV/TL), which normalizes the LV mass to the body size, sham mice showed a ratio of 4.7±0.1 and 3.8±0.1 mg/mm for morphometric and MRI measurements, respectively, and TAC mice showed a ratio of 6.5±0.4 and 5.4±0.3, respectively, demonstrating a clearly different cardiac phenotype between both groups (p<0.05, Fig. 2). Detailed cardiac functional parameters and LV mass measurements for the sham and TAC groups are summarized in Table 1.

Intraobserver, Interobserver and Interexperiment Variability of MRI Data

The mean±SD values of all morphometric data as well as the Bland-Altman analysis were obtained for the 29 animals studied. Detailed results are displayed in Table 2 and Fig. 3. We did not find statistically significant differences between the mean values of LV mass, LV/TL ratio, LV EDV, LV ESV, LV SV and LV EF when comparing the various sets of data (p>0.05).

As expected, the SDD, and hence the limits of agreement, were smaller for all parameters in the intraobserver study, whereas the least clustered data were found in the interexperiment study, with similar to larger confidence interval compared to the interobserver study.

Using the Bland and Altman analysis, high reproducibility was found for LV mass, LV/TL and EDV, with a notably low intraobserver CoV of 5.4 % for all these parameters and CoV <12 % in the interexperiment study, suggesting that these can effectively be used in longitudinal studies. Good agreement was found for EF, with a CoV between 14.7 % in the interobserver study and 15.5 % in the interexperiment study. The small volumes suffered the most variability, with intermodality CoV between 15.2 and 20.9 % for ESV and SV, which implies that they are more difficult to quantify accurately and could be of limited value when measured during repeated acquisitions.

Fig. 4 *Scatterplots* showing the intraobserver, interobserver and interexperiment correlations between two readings for LV/TL, EDV, ESV, SV and EF. Our linear regression analysis shows an excellent correlation for all intraobserver data, but moderate correlation in SV and EF for interobserver data and in SV for interexperiment data. The regression line is given with a 95 % confidence interval (*dotted lines*). R-squares and p values are reported in the *left upper corner* of each graph

Linear Regression Analysis

Linear regression analysis for all mice revealed an adequate intraobserver, interobserver and interexperiment correlation for LV/TL, EDV, ESV and EF with R-square ranging between 0.67 and 0.95. Correlation for SV was the weakest of all parameters, with R-square between 0.30 (interobserver study) and 0.67 (intraobserver study). The line of best fit intercepted the origin for most measurements, and when not, the correlation remained significant, with a b_0 significantly different from zero. The scatter plots with individual regression line, 95 % confidence interval, R-squares and corresponding p-values are provided in Fig. 4.

Correlation Between In Vivo MRI and Ex Vivo Morphometric LV Mass Measurements

We demonstrated a strong correlation between LV mass measurements by LV mass weighing or high-field CMR imaging (data set 2), with a Pearson correlation (r) of 0.92 for both LV mass and LV/TL ratio (p<0.05, Fig. 5). Of note, MRI data in absolute values were always smaller than morphometric data.

Discussion

In cardiovascular imaging, variations within and between observers and between different acquisitions remain an important issue when evaluating in vivo data. This is particularly relevant when experimental groups are studied longitudinally to test a new hypothesis.

Up to now, high-frequency echocardiography remained the most widely used technique to characterize the cardiac phenotype of rodents. Although few data are available in the literature on its reproducibility [22–25], it is generally accepted that its intra- and interobserver variability is low for most ventricular measurements (<20 %, [26]). However, it is also known that this method is less efficient in the presence of abnormal ventricular geometry and heterogeneous regional myocardial function [26–28] as it is often the case in animal models of cardiovascular diseases.

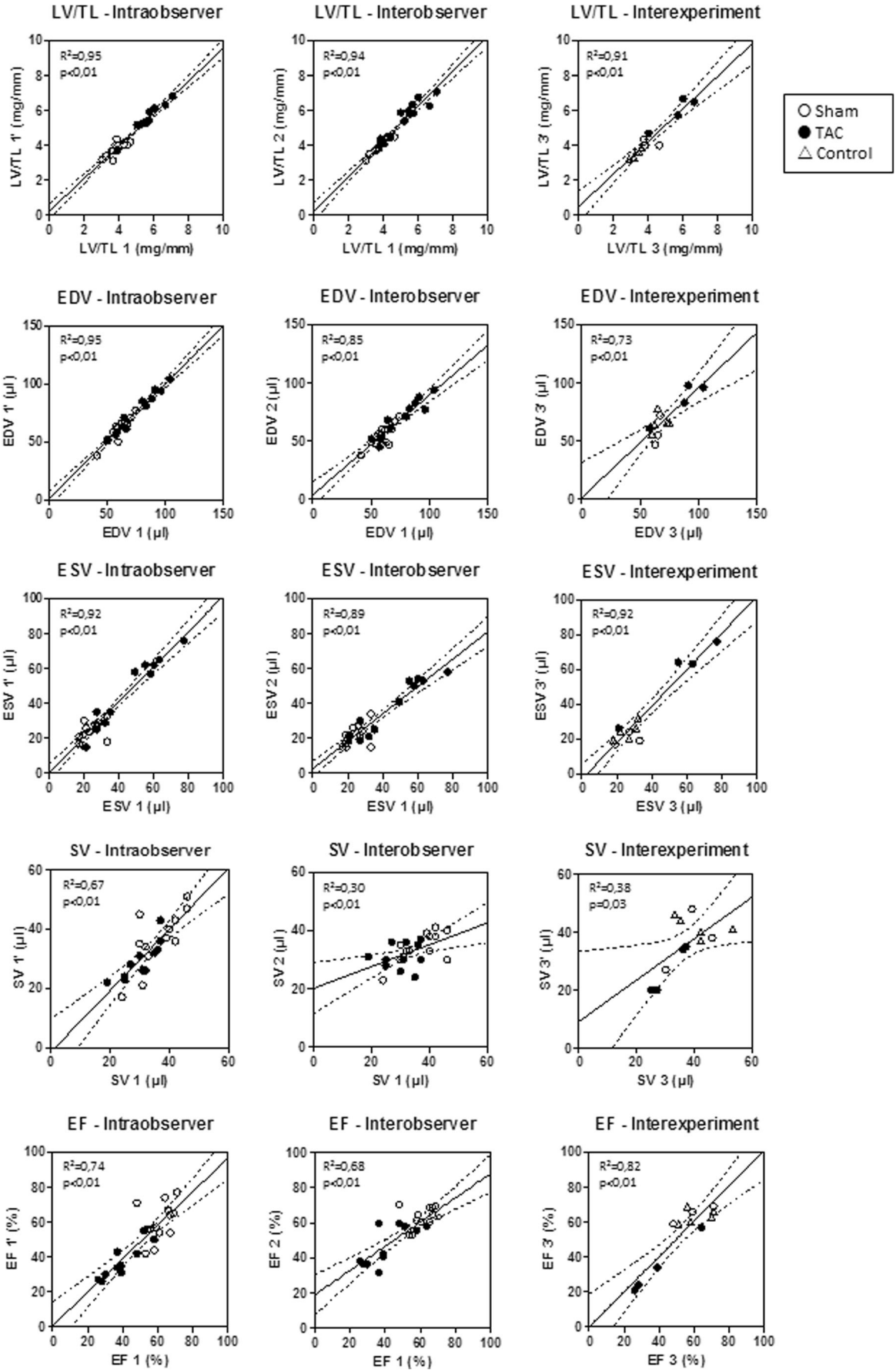
LV/TL - Intraobserver
R²=0,95
p<0,01
LV/TL 1' (mg/mm)
LV/TL 1 (mg/mm)
LV/TL - Interobserver
R²=0,94
p<0,01
LV/TL 2 (mg/mm)
LV/TL 1 (mg/mm)
LV/TL - Interexperiment
R²=0,91
p<0,01
LV/TL 3' (mg/mm)
LV/TL 3 (mg/mm)
Sham
TAC
Control
EDV - Intraobserver
R²=0,95
p<0,01
EDV 1' (µl)
EDV 1 (µl)
EDV - Interobserver
R²=0,85
p<0,01
EDV 2 (µl)
EDV 1 (µl)
EDV - Interexperiment
R²=0,73
p<0,01
EDV 3' (µl)
EDV 3 (µl)
ESV - Intraobserver
R²=0,92
p<0,01
ESV 1' (µl)
ESV 1 (µl)
ESV - Interobserver
R²=0,89
p<0,01
ESV 2 (µl)
ESV 1 (µl)
ESV - Interexperiment
R²=0,92
p<0,01
ESV 3' (µl)
ESV 3 (µl)
SV - Intraobserver
R²=0,67
p<0,01
SV 1' (µl)
SV 1 (µl)
SV - Interobserver
R²=0,30
p<0,01
SV 2 (µl)
SV 1 (µl)
SV - Interexperiment
R²=0,38
p=0,03
SV 3' (µl)
SV 3 (µl)
EF - Intraobserver
R²=0,74
p<0,01
EF 1' (%)
EF 1 (%)
EF - Interobserver
R²=0,68
p<0,01
EF 2 (%)
EF 1 (%)
EF - Interexperiment
R²=0,82
p<0,01
EF 3' (%)
EF 3 (%)

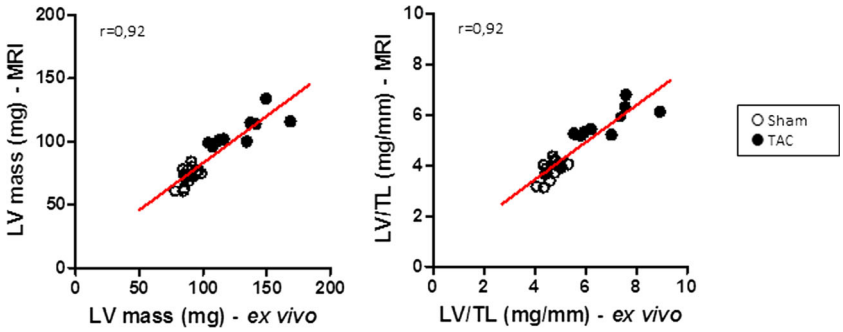

Fig. 5 Correlation between in vivo MRI data and ex vivo morphometric data in terms of LV mass and LV/TL ratio. MRI data are issued from data set 1′

Approaches such as echocardiography using geometrical assumptions to evaluate left ventricular function are not as accurate as data coming from a full volume acquisition, as it is the gold standard in CMR imaging [15]. In a rat model of myocardial infarction, Stuckey et al. showed that 2D echo was indeed less reproducible than 11.7 T MRI [13] in a vertical bore magnet acquiring 28–40 frames per heart cycle.

Studies comparing measurements obtained by echocardiography and MRI in a model are scarce [13, 28], but overall, they suggest that end-diastolic dimensions and LV wall thickness are poorly correlated. This could be at least in part explained by the better delineation of cardiac trabeculations in CMR imaging and better temporal resolution [27]. Similarly, studies comparing left ventricular function in mice by MRI or conductance microcatheter (Millar) have shown a striking underestimation of absolute volumetric values with the catheter method [29, 30] influenced by the calibration technique used [30]. These pitfalls further suggest that it is not wise to compare LV measurements obtained with different techniques in various experimental groups.

Development of ultra-high-field MRI systems (≥7.0 T) over the past decade has brought new perspectives in small animal imaging. As there is a direct relationship between the main field strength (B_0) and the signal-to-noise ratio (S/N), higher field provides better imaging quality and improves spatial and temporal resolution or acquisition speed. Hence, most pioneering CMR laboratories currently work on 7 or 9 T systems [9], and they are likely to transition to even higher fields in the near future. If some reproducibility data on CMR in rodents are available, they mainly report very small numbers of animals ($n<10$) [10–12], including rats [12, 13], field strengths ≤7 T [14] or vertical bores [11–13], the latter representing a less physiological environment. Overall, this does not really reflect the current use of ultra-high-field MRI for the characterization of experimental models in cardiovascular research. Moreover, interexperiment variability is usually not evaluated in most studies, including the work of Heijman et al. [14] reporting the most sizable number of mice ($n=22$) at 6.3 T. Therefore, we believe that our reproducibility data obtained with a horizontal bore at 11.7 T on a group of more than 25 mice bring additional material for the validation of the technique.

In our study, purposedly including healthy mice and a model of hypertrophic cardiomyopathy, intraobserver, interobserver and interexperiment reproducibility was good for LV mass, LV/TL and EDV (CoV between 5.4 and 11.8 %). These results are consistent with the few data available in the experimental field [10–15], although the use of different statistical tests does not allow a thorough comparison. Coefficients of variability remain higher than those obtained in humans [31]. If the reproducibility of ESV, SV and EF is less satisfactory, various factors may account for these differences. First, contour tracings in the basal and apical sections of the heart are often subject to interpretation at the time of post-processing because myocardial limits are less clearly visible at these levels. Secondly, at least when studying interexperiment variability, an additional potential source of error in the determination of volumes could have been introduced by the partial volume effect due to a finite slice thickness. Finally, and above all, there was an important scale effect: any tiny variation in measurements had enormous repercussions on the reproducibility of the data, as it related to very small volumes (μl). This explains why the smallest volumes, especially the SV, suffered the most variability. This highlights the need to develop stronger sequences to adequately measure SV and cardiac output in mice. In particular, a phase-contrast angiography sequence applied on the ascending aorta could be more appropriate for direct measurement of the SV and, subsequently, the EF [32].

When morphometric and CMR imaging LV measurements were compared, both showed a strong correlation and were able to demonstrate similar differences in LV mass or LV/TL between our experimental groups. However, LV mass estimated by CMR was consistently smaller in absolute values than those obtained ex vivo. The 1-week delay between MRI examination and sacrifice for morphometric evaluation could in part account for this discrepancy. However, this is also very likely related to the great accuracy of CMR post-processing, allowing to exclude intraventricular blood and tissues not belonging to the LV from the analysis, whereas those may have been mistakenly included in the morphometric measurements.

Conclusions

This study showed that the mouse LV systolic function can be assessed on an 11.7 T MRI scanner, with an excellent reproducibility of LV mass and end-diastolic volumes analysis, allowing longitudinal phenotypic evaluation of animals with healthy or hypertrophic myocardium. Furthermore, in vivo LV mass MRI measurements were constantly in line with ex vivo morphometric data, bringing evidence that high-field CMR imaging is not only reproducible but also accurate.

Development of new CMR imaging sequences remains a great challenge for the future, as it will allow more detailed non-invasive characterizations of animal models. Here, we highlight the need to interpret CMR data by taking into account their shortcomings, focusing on LV mass and LV EDV as parameters that are not only the most reproducible but also the most relevant in various pathophysiological conditions such as cardiac remodeling and hypertrophy.

Acknowledgments We thank Julie Magat and Hassan Jassar for their assistance during the MRI manipulations. This work was supported by grants from the Fonds de la Recherche Scientifique FRS-FNRS, the Foundation Saint-Luc and the Belgian National Foundation for Research in Pediatric Cardiology.

Conflict of Interest No potential conflicts of interest were disclosed.

Animal Studies All institutional and national guidelines for the care and use of laboratory animals were followed and approved by the appropriate institutional committees. No human studies were carried out by the authors for this article.

References

1. Mozaffarian, D., Benjamin, E. J., Go, A. S., Arnett, D. K., Blaha, M. J., Cushman, M., de Ferranti, S., Després, J., Fullerton, H. J., Howard, V. J., Huffman, M. D., Judd, S. E., Kissela, B. M., Lackland, D. T., Lichtman, J. H., Lisabeth, L. D., Liu, S., Mackey, R. H., Matchar, D. B., McGuire, D. K., Mohler, E. R., 3rd, Moy, C. S., Muntner, P., Mussolino, M. E., Nasir, K., Neumar, R. W., Nichol, G., Palaniappan, L., Pandey, D. K., Reeves, M. J., Rodriguez, C. J., Sorlie, P. D., Stein, J., Towfighi, A., Turan, T. N., Virani, S. S., Willey, J. Z., Woo, D., Yeh, R. W., & Turner, M. B. (2015). Heart disease and stroke statistics—2015 update: a report from the American Heart Association. *Circulation, 131*(4), e29–e322.
2. Schneider, J. E., Wiesmann, F., Lygate, C. A., & Neubauer, S. (2006). How to perform an accurate assessment of cardiac function in mice using high-resolution magnetic resonance imaging. *Journal of Cardiovascular Magnetic Resonance, 8*, 693–701.
3. Vallée, J. P., Ivancevic, M. K., Nguyen, D., Morel, D. R., & Jaconi, M. (2004). Current status of cardiac MRI in small animals. *Magnetic Resonance Materials in Physics, Biology and Medicine, 17*(3–6), 149–156.
4. Epstein, F. H. (2007). MR in mouse models of cardiac disease. *NMR in Biomedicine, 20*(3), 238–255.
5. Price, A. N., Cheung, K. K., Cleary, J. O., Campbell, A. E., Riegler, J., & Lythgoe, M. F. (2010). Cardiovascular magnetic resonance imaging in experimental models. *The Open Cardiovascular Medicine Journal, 4*, 278–292.
6. Vandsburger, M. H., & Epstein, F. H. (2011). Emerging MRI methods in translational cardiovascular research. *Journal of Cardiovascular Translational Research, 4*(4), 477–492.
7. Akki, A., Gupta, A., & Weiss, R. G. (2013). Magnetic resonance imaging and spectroscopy of the murine cardiovascular system. *American Journal of Physiology Heart and Circulation Physiology, 304*(5), H633–H648.
8. Meßner, N. M., Zöllner, F. G., Kalayciyan, R., & Schad, L. R. (2014). Pre-clinical functional magnetic resonance imaging part II: the heart. *Zeitschrift für Medizinische Physik, 24*(4), 307–322.
9. Kraff, O., Fischer, A., Nagel, A. M., Mönninghoff, C., & Ladd, M. E. (2015). MRI at 7 tesla and above: demonstrated and potential capabilities. *Journal of Magnetic Resonance Imaging, 41*(1), 13–33.
10. Ruff, J., Wiesmann, F., Hiller, K. H., Voll, S., von Kienlin, M., Bauer, W. R., Rommel, E., Neubauer, S., & Haase, A. (1998). Magnetic resonance microimaging for noninvasive quantification of myocardial function and mass in the mouse. *Magnetic Resonance in Medicine, 40*, 43–48.
11. Schneider, J. E., Cassidy, P. J., Lygate, C., Tyler, D. J., Wiesmann, F., Grieve, S. M., Hulbert, K., Clarke, K., & Neubauer, S. (2003). Fast, high-resolution in vivo cine magnetic resonance imaging in normal and failing mouse hearts on a vertical 11.7 T system. *Journal of Magnetic Resonance Imaging, 18*, 691–701.
12. Tyler, D. J., Lygate, C. A., Schneider, J. E., Cassidy, P. J., Neubauer, S., & Clarke, K. (2006). CINE-MR imaging of the normal and infarcted rat heart using an 11.7 T vertical bore MR system. *Journal of Cardiovascular Magnetic Resonance, 8*, 327–333.
13. Stuckey, D. J., Carr, C. A., Tyler, D. J., & Clarke, K. (2008). Cine-MRI versus two-dimensional echocardiography to measure in vivo left ventricular function in rat heart. *NMR in Biomedicine, 21*(7), 765–772.
14. Heijman, E., Aben, J. P., Penners, C., Niessen, P., Guillaume, R., van Eys, G., Nicolay, K., & Strijkers, G. J. (2008). Evaluation of manual and automatic segmentation of the mouse heart from CINE MR images. *Journal of Magnetic Resonance Imaging, 27*(1), 86–93.
15. van de Weijer, T., van Ewijk, P. A., Zandbergen, H. R., Slenter, J. M., Kessels, A. G., Wildberger, J. E., Hesselink, M. K., Schrauwen, P., Schrauwen-Hinderling, V. B., & Kooi, M. E. (2012). Geometrical models for cardiac MRI in rodents: comparison of quantification of left ventricular volumes and function by various geometrical models with a full-volume MRI data set in rodents. *American Journal of Physiology Heart and Circulation Physiology, 302*(3), H709–H715.
16. Wiesmann, F., Ruff, J., Engelhardt, S., Hein, L., Dienesch, C., Leupold, A., Illinger, R., Frydrychowicz, A., Hiller, K. H., Rommel, E., Haase, A., Lohse, M. J., & Neubauer, S. (2001). Dobutamine-stress magnetic resonance microimaging in mice: acute changes of cardiac geometry and function in normal and failing murine hearts. *Circulation Research, 88*, 563–569.
17. Rockman, H. A., Ross, R. S., Harris, A. N., Knowlton, K. U., Steinhelper, M. E., Field, L., Ross, J., & Chien, K. R. (1991). Segregation of atrial specific and inducible expression of an ANF transgene in an in vivo murine model of cardiac hypertrophy. *Proceedings of the National Academy of Sciences of the United States of America, 88*, 8277–8281.
18. Hu, P., Zhang, D., Swenson, L., Chakrabarti, G., Abel, E. D., & Litwin, S. E. (2003). Minimally invasive aortic banding in mice: effects of altered cardiomyocyte insulin signaling during pressure overload. *American Journal of Physiology Heart and Circulation Physiology, 285*(3), H1261–H1269.
19. Kober, F., Iltis, I., Cozzone, P. J., & Bernard, M. (2004). Cine-MRI assessment of cardiac function in mice anesthetized with ketamine/

xylazine and isoflurane. *Magnetic Resonance Materials in Physics, Biology and Medicine, 17*(3–6), 157–161.

20. Heiberg, E., Sjögren, J., Ugander, M., Carlsson, M., Engblom, H., & Arheden, H. (2010). Design and validation of segment-freely available software for cardiovascular image analysis. *BMC Medical Imaging, 10*, 1.
21. Bland, J. M., & Altman, D. G. (1986). Statistical methods for assessing agreement between two methods of clinical measurement. *Lancet, 1*, 307–310.
22. Hoit, B. D., Khoury, S. F., Kranias, E. G., Ball, N., & Walsh, R. A. (1995). In vivo echocardiographic detection of enhanced left ventricular function in gene-targeted mice with phospholamban deficiency. *Circulation Research, 77*(3), 632–637.
23. Tanaka, N., Dalton, N., Mao, L., Rockman, H. A., Peterson, K. L., Gottshall, K. R., Hunter, J. J., Chien, K. R., & Ross, J., Jr. (1996). Transthoracic echocardiography in models of cardiac disease in the mouse. *Circulation, 94*(5), 1109–1117.
24. Yang, X. P., Liu, Y. H., Rhaleb, N. E., Kurihara, N., Kim, H. E., & Carretero, O. A. (1999). Echocardiographic assessment of cardiac function in conscious and anesthetized mice. *American Journal of Physiology Heart and Circulation Physiology, 277*, H1967–H1974.
25. Collins, K. A., Korcarz, C. E., Shroff, S. G., Bednarz, J. E., Fentzke, R. C., Lin, H., Leiden, J. M., & Lang, R. M. (2001). Accuracy of echocardiographic estimates of left ventricular mass in mice. *American Journal of Physiology Heart and Circulation Physiology, 280*(5), H1954–H1962.
26. Ram, R., Mickelsen, D. M., Theodoropoulos, C., & Blaxall, B. C. (2011). New approaches in small animal echocardiography: imaging the sounds of silence. *American Journal of Physiology Heart and Circulation Physiology, 301*(5), H1765–H1780.
27. Ghanem, A., Roll, W., Hashemi, T., Dewald, O., Djoufack, P. C., Fink, K. B., Schrickel, J., Lewalter, T., Luderitz, B., & Tiemann, K. (2006). Echocardiographic assessment of left ventricular mass in neonatal and adult mice: accuracy of different echocardiographic methods. *Echocardiography, 23*, 900–907.
28. Amundsen, B. H., Ericsson, M., Seland, J. G., Pavlin, T., Ellingsen, Ø., & Brekken, C. (2011). A comparison of retrospectively self-gated magnetic resonance imaging and high-frequency echocardiography for characterization of left ventricular function in mice. *Laboratory Animal, 45*(1), 31–37.
29. Jacoby, C., Molojavyi, A., Flögel, U., Merx, M. W., Ding, Z., & Schrader, J. (2006). Direct comparison of magnetic resonance imaging and conductance microcatheter in the evaluation of left ventricular function in mice. *Basic Research in Cardiology, 101*(1), 87–95.
30. Nielsen, J. M., Kristiansen, S. B., Ringgaard, S., Nielsen, T. T., Flyvbjerg, A., Redington, A. N., & Bøtker, H. E. (2007). Left ventricular volume measurement in mice by conductance catheter: evaluation and optimization of calibration. *American Journal of Physiology Heart and Circulation Physiology, 293*(1), H534–H540.
31. Luijnenburg, S. E., Robbers-Visser, D., Moelker, A., Vliegen, H. W., Mulder, B. J., & Helbing, W. A. (2010). Intra-observer and interobserver variability of biventricular function, volumes and mass in patients with congenital heart disease measured by CMR imaging. *International Journal of Cardiovascular Imaging, 26*(1), 57–64.
32. Janiczek, R. L., Blackman, B. R., Roy, R. J., Meyer, C. H., Acton, S. T., & Epstein, F. H. (2011). Three-dimensional phase contrast angiography of the mouse aortic arch using spiral MRI. *Magnetic Resonance in Medicine, 66*, 1382–1390.